This is a pre-peer reviewed version of the manuscript published in:

Electrochemistry Communications, 2015, Volume 54, Pages 14-17

(DOI: 10.1016/j.elecom.2015.02.012)

Monitoring Charge Transfer at Polarisable Liquid/Liquid Interfaces Employing Time-Resolved Raman Spectroelectrochemistry.

D. Ibañez[1], D. Plana[2], A. Heras[1], D.J. Fermín[2], A. Colina[1,*].

1. *Department of Chemistry, Universidad de Burgos, Pza. Misael Bañuelos s/n, E-09001 Burgos, Spain.*
2. *School of Chemistry, University of Bristol, Cantocks Close, Bristol BS8 1TS, U.K.*

* Corresponding author: acolina@ubu.es, Tel: +34-947258817, Fax: +34-947258831.

Abstract

In-situ Raman spectroscopy is implemented for the first time to monitor dynamic charge transfer processes at polarisable interfaces between two immiscible electrolyte solutions (ITIES) in real time. A custom-designed new electrochemical cell is described which allows probing the Raman signals of ferroin ions as a function of the potential applied across the water|1,2-dichlorobenzene (DCB) interface. This approach is also used for investigating the heterogeneous electron transfer reaction involving

dimethylferrocene in DCB and potassium hexacyanoferrate (II/III) in the aqueous phase. The evolution of the Raman signals during potentiodynamic measurements is recorded in real-time with a resolution of a few seconds.

Keywords

Liquid/liquid interfaces; ion transfer; electron transfer; In-situ Raman spectroscopy.

1. Introduction

In-situ spectroscopic techniques have revealed a wealth of information about the structure and reaction mechanisms taking place at polarisable interfaces between two immiscible electrolyte solutions (ITIES) [1]. The complexity of probing interfacial processes lies on the buried nature of these interfaces, requiring the coupling of spectroscopic signals with potential perturbations [2–6], or the use of non-linear optical techniques [7–9]. Although Raman spectroscopy has already been used to probe interfacial confined species, the majority of the work has been carried out in the absence of external polarisation [10,11]. More recently, Raman responses as a function of the Galvani potential difference across the ITIES have been reported under stationary conditions [12,13]. In this report, we described the first *in-situ* Raman studies at the polaraisable ITIES under potentiodynamic conditions in real time. A purposely built low-volume four-electrode cell is presented which enables monitoring Raman responses associated with ion transfer and heterogeneous electron transfer across the water|1,2-dichlorobenzene (DCB) interface. A clear correlation between spectroscopic and electrochemical responses is shown, demonstrating a high level of sensitivity and time-resolution.

2. Material and methods

All reagents employed were analytical grade or higher. The organic phase supporting electrolyte was bis(triphenylphosphoranylidene) ammonium tetrakis(pentafluoro) phenylborate (BTPPATPBF_{20}) [14]. In order to facilitate the use of low volumes, DCB electrolyte solution was gelled employing high molecular weight polyvinylchloride (PVC) following the methodology reported in [15]. The aqueous electrolyte solutions were prepared using high purity de-ionised water (MilliQ gradient A10 system, Millipore).

Electrochemical measurements were carried out at room temperature using an AUTOLAB PGSTAT20 potentiostat (Eco Chemie Autolab) in four-electrode mode. The potential scale in this work corresponds to the potential difference between the reference electrode in the aqueous phase (so-called sensor electrode) and the reference electrode in the organic phase ($\Delta\phi = E_{ref,water} - E_{ref,organic}$). Raman spectra were obtained using a Confocal Raman Voyage (BWTEK). A laser wavelength of 532 nm with a power of 15 mW was employed to obtain the spectra, using a 20× objective. Further details about the dynamic spectroelectrochemical Raman system have been previously reported [16,17]. An XYZ piezoelectric positioner (Newport 271) controlled by a Newport motion controller (Newport, ESP 301) was used to focus the laser beam with micrometric resolution.

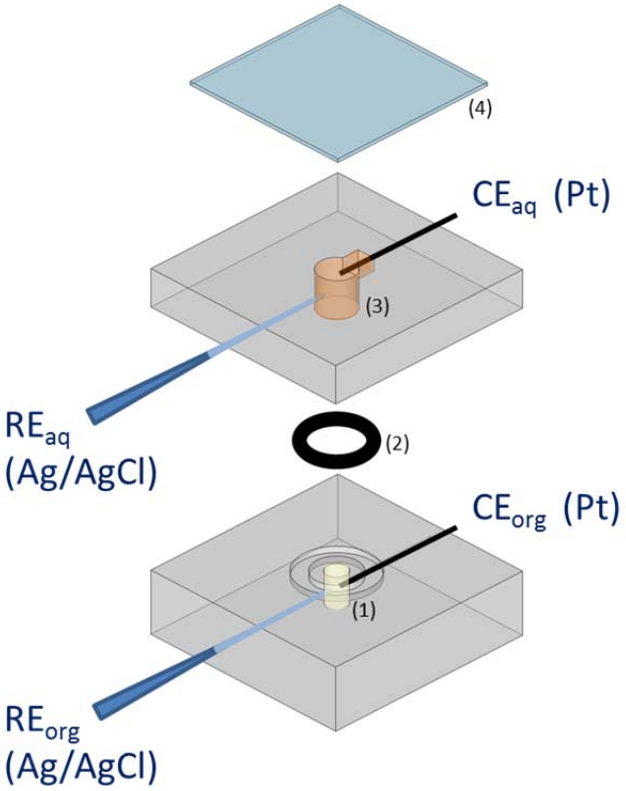

Figure.1. Schematic design of the 4-electrode cell for dynamic Raman spectroelectrochemistry, featuring: the organic gel compartment (1), O-ring (2), the aqueous electrolyte compartment (3), and quartz window (4).

A schematic representation of the polytetrafluoroethylene (PTFE) built 4-electrode cell is shown in Figure 1. The organic phase compartment (1) was 7 mm in depth and 3 mm in diameter, while the aqueous electrolyte compartment (3) consisted of a cylindrical hole of 6 mm diameter and 6 mm long. The O-ring (2) was used to prevent electrolyte leakage while the reference and counter electrodes in both phases were placed through small holes at the side of the corresponding compartments. This configuration ensured a clear optical path for the laser through the quartz window (4) on top of the cell.

3. Results and Discussion

3.1. $[Fe(phen)_3]^{2+}$ transfer across the water|DCB interface.

The spectroelectrochemical cell composition used was: Ag (s) | AgCl (s) | 1 mM BTPPACl + 10 mM LiCl (aq) | 18 mM $BTPPATPBF_{20}$ + 2% (w/w) PVC (DCB/THF, 50%) || 25 mM $[Fe(phen)_3]^{2+}$ + 0.1 M LiCl (aq) | AgCl (s) | Ag (s); where the double bar denotes the polarisable interface. Two consecutive linear sweep voltammograms recorded at 0.005 V s^{-1}, focusing the laser in the aqueous and in the organic phases, are displayed in Figure 2a. The current peak located at $\Delta\phi$ ~ +0.30 V is associated with the transfer of $[Fe(phen)_3]^{2+}$ from the aqueous to the organic electrolyte. Characteristic Raman spectra recorded during the potential cycle while the laser is focused in the aqueous side of the interface are shown in Figure 2b. The two intense Raman peaks at 1457 and 1517 cm^{-1} correspond to in-plane stretching vibration of the phenanthroline ring [18]. Figure 2c shows a similar set of spectra but focusing the laser in the organic side of the interface. The results clearly show that as the potential is swept positively, the intensity of the Raman responses decreases in the aqueous side of the interface while concomitantly increasing in the organic side.

The interplay between the signals in the aqueous and organic phases is clearly visualised in Figures 2d and 2e. Little changes in the Raman intensity are observed at potentials more negative than 0.00 V. These results also demonstrate that the cathodic current at negative $\Delta\phi$ are associated with the transfer of supporting ionic species in the background electrolyte (most probably Cl^- from water to DCB). Figure 2f correlates the faradaic charge obtained from integration of the linear sweep voltammetry and the Raman intensity variation (ΔI_{Raman}) at 1457 cm^{-1} registered when the laser was focused on the organic phase. From the slope of the trend in Figure 2f, it can be estimated that Raman responses are capable of detecting changes in the interfacial population of $[Fe(phen)_3]^{2+}$ close to 4.6×10^{-9} mol/Raman intensity unit.

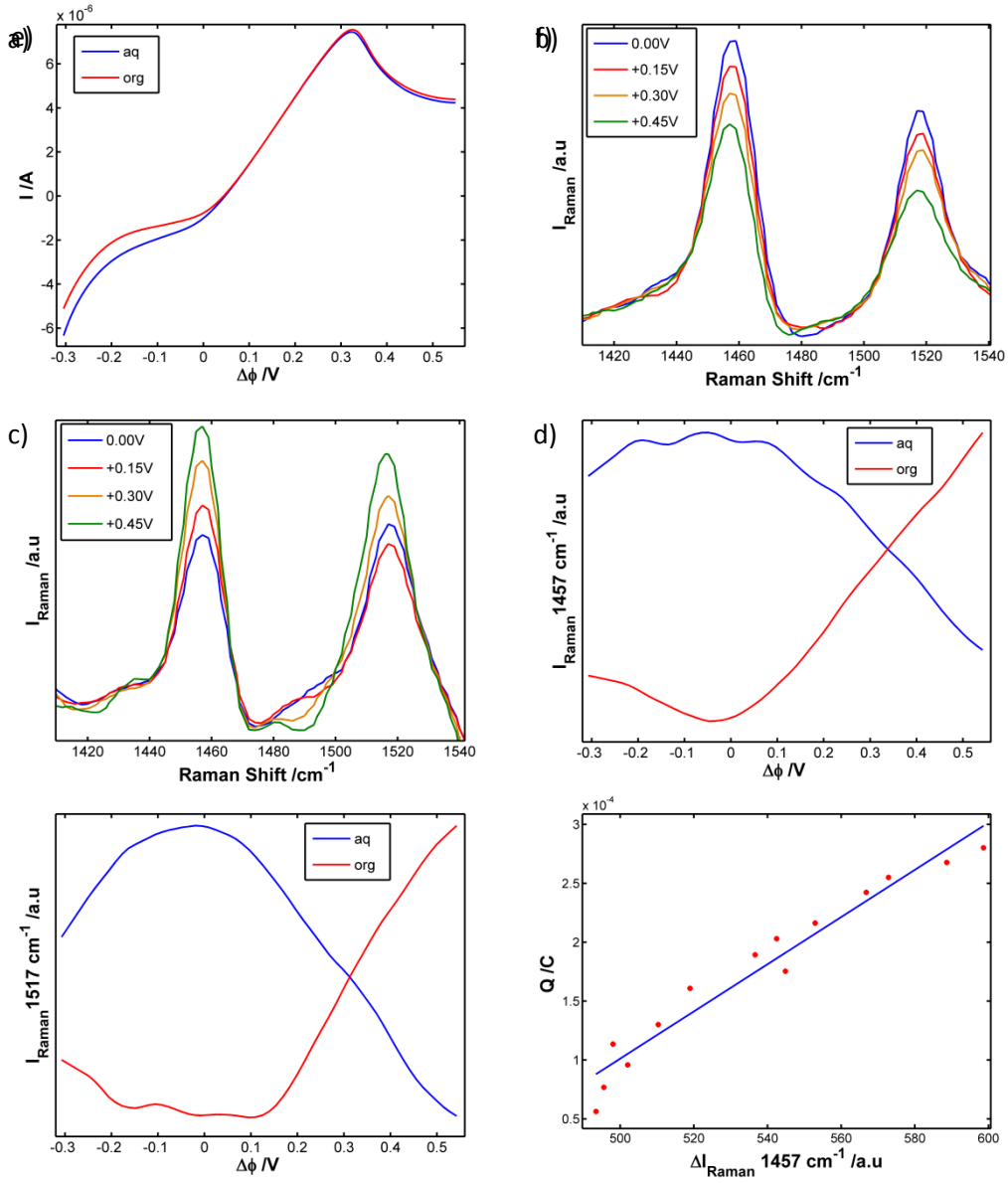

Figure. 2. (a) Linear sweep voltammograms recorded at 0.005 V s^{-1} starting from $\Delta\phi$=-0.30 V. Two consecutive cycles were recorded in order to measure Raman spectra with the laser focused in the aqueous and organic sides of the interface. (b) Selected Raman spectra recorded in real-time, integration time: 2.8 s, at various potentials with the laser focused in the aqueous and (c) organic side of the interface. (d) Evolution of the Raman intensity at 1457 cm^{-1} and (e) 1517 cm^{-1} during the potential cycle. (f) Raman intensity variation (ΔI_{Raman}) at 1457 cm^{-1} from the organic side as a function of the faradaic charge.

3.2. Heterogeneous electron transfer reaction.

A second test case investigated is the heterogeneous electron transfer between hexacyanoferrate (III) and DMFC. The spectroelectrochemical cell composition used was: Ag(s) | AgCl (s) | 1 mM BTPPACl + 10 mM LiCl (aq) | 5 mM $BTPPATPBF_{20}$ + 25 mM DMFc + 2% (w/w) PVC (DCB/THF, 50%) || 25 mM $K_4[Fe(CN)_6]$ + 25 mM $K_3[Fe(CN)_6]$ + 0.1 M LiCl (aq) | AgCl(s) | Ag (s). The Raman spectra shown in Figure 3a feature hexacyanoferrate (II) bands at 2055 and 2093 cm^{-1}, as well as a band at 2132 cm^{-1} associated with hexacyanoferrate (III). These bands correspond to the C≡N stretching vibration which is sensitive to the oxidation state of Fe [19,20]. At $\Delta\phi$ < +0.30 V, the intensity of the Raman signals is weakly dependent on the potential difference between the two reference electrodes. As $\Delta\phi$ is increased above +0.30 V, a clear increase in the intensity of the bands associated with hexacyanoferrate (II) is observed concomitantly with a decrease of the hexacyanoferrate (III) response (Figure 3b). These changes in the Raman signal are indicative of the heterogeneous electron transfer response involving DMFC in the organic solution. Figure 3c also shows a direct relationship between the band at 2132 cm^{-1} and the faradaic charge associated with the oxidation of DMFC. In this experiment Raman responses are capable of detecting changes in the interfacial population of hexacyanoferrate (III) close to $1.9x10^{-7}$ mol/Raman intensity unit. The spectral response was much more sensitive for the ion transfer experiment using $[Fe(phen)_3]^{2+}$ than for the electron transfer reaction using hexacyanoferrate. $[Fe(phen)_3]^{2+}$ shows an absorption band peak at 505 nm, whereas hexacyanoferrate (III) absorbs at 420 nm. Thus, in the ion transfer experiment resonance Raman is taking place, improving the sensitivity of the technique.

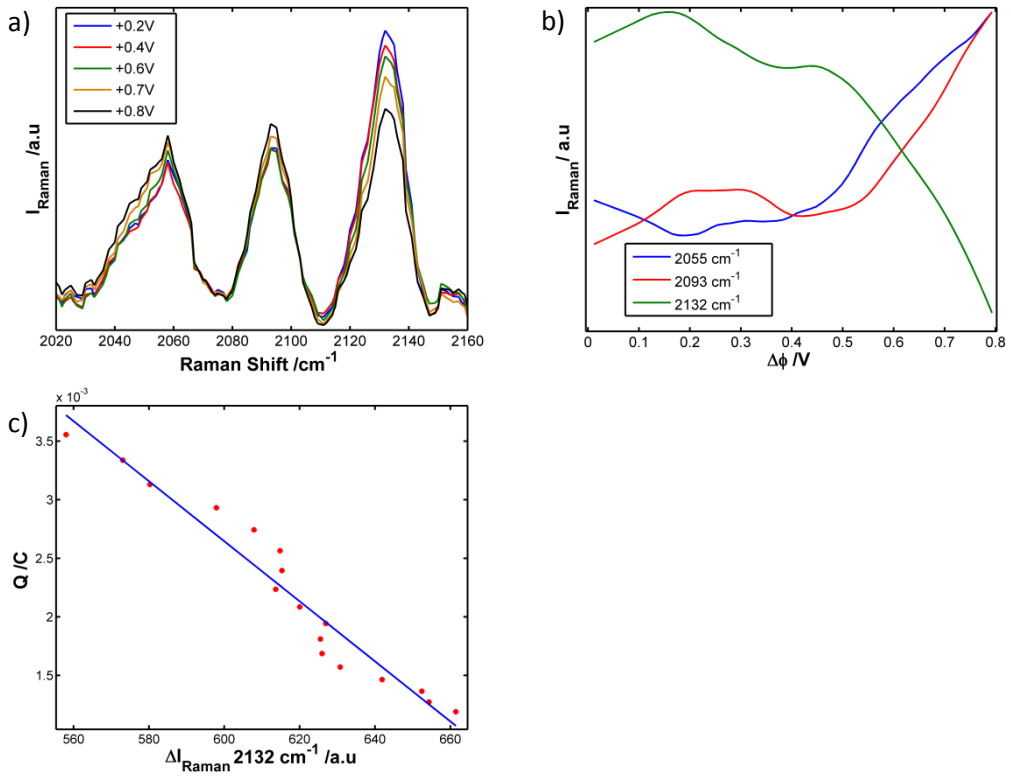

Figure.3. (a) Raman spectra obtained focusing the laser in the aqueous side of the interface while sweeping the $\Delta\phi$ at 0.001 V s^{-1}. (b) Evolution of the bands at 2055, 2093 and 2132 cm^{-1} as a function of $\Delta\phi$, integration time: 12.8 s. (c) ΔI_{Raman} at 2132 cm^{-1}, corresponding to hexacyanoferrate (III), as a function of the faradaic charge associated with the heterogeneous electron transfer process.

4. Conclusions

A new Raman spectroelectrochemical cell has been developed that allows studying ion and heterogeneous electron transfer at polarisable ITIES *in-situ* and in potentiodynamic conditions. By carefully positioning the focal point of the excitation laser, the depletion of the ion probe at the aqueous side of the interface and the corresponding accumulation in the organic side can be detected in real time. Furthermore, we were able to detect changes in the C≡N stretching vibration of hexacyanoferrate (II/III) during the heterogeneous electron transfer from DMFC. This

exquisite spectral-temporal resolution can be exploited in more complicated systems featuring partially solvated species as well as nanoparticle decorated ITIES.

Acknowledgments

The financial support made available by the Junta de Castilla y León (GR71, BU349-U13) and Ministerio de Economía y Competitividad (CTQ2010-17127) is gratefully acknowledged. D.I. thanks Ministerio de Economia y Competitividad for his predoctoral FPI fellowship. D.P. and D.J.F. acknowledge financial support from the EPSRC (grant EP/K007025/1).

References

[1] David J. Fermín, Linear and Non-linear Spectroscopy at the Electrified Liquid/Liquid Interface, in: R.C. Alkire, D.M. Kolb, J. Lipkowski, P.N. Ross (Eds.), Adv. Electrochem. Sci. Eng., WILEY-VCH Verlag GmbH & Co. KGaA, Weinheim, 2006: pp. 127–162.

[2] Z. Ding, D.J. Fermın, P.-F. Brevet, H.H. Girault, Spectroelectrochemical approaches to heterogeneous electron transfer reactions at the polarised water 1,2-dichloroethane interfaces, J. Electroanal. Chem. 458 (1998) 139–148.

[3] H. Nagatani, R.A. Iglesias, D.J. Fermín, P.-F. Brevet, H.H. Girault, Adsorption behavior of charged zinc porphyrins at the water/1,2-dichloroethane interface studied by potential modulated fluorescence spectroscopy, J. Phys. Chem. B. 104 (2000) 6869–6876.

[4] H. Nagatani, H. Watarai, Direct Spectrophotometric Measurement of Demetalation Kinetics of 5,10,15,20-Tetraphenylporphyrinatozinc(II) at the Liquid-Liquid Interface by a Centrifugal Liquid Membrane Method, Anal. Chem. 70 (1998) 2860–2865.

[5] A. Martínez, A. Colina, R.A.W. Dryfe, V. Ruiz, Spectroelectrochemistry at the liquid|liquid interface: Parallel beam UV–vis absorption, Electrochim. Acta. 54 (2009) 5071–5076.

[6] D. Izquierdo, A. Martinez, A. Heras, J. Lopez-Palacios, V. Ruiz, R.A.W. Dryfe, A. Colina, Spatial Scanning Spectroelectrochemistry. Study of the Electrodeposition of Pd Nanoparticles at the Liquid/Liquid Interface, Anal. Chem. 84 (2012) 5723–5730.

[7] D.A. Higgins, R.M. Corn, Second harmonic generation studies of adsorption at a liquid-liquid electrochemical interface, J. Phys. Chem. 97 (1993) 489–493.

[8] K.B. Eisenthal, Liquid Interfaces Probed by Second-Harmonic and Sum-Frequency Spectroscopy, Chem. Rev.. 96 (1996) 1343–1360.

[9] G.L. Richmond, Molecular bonding and interactions at aqueous surfaces as probed by vibrational sum frequency spectroscopy, Chem. Rev. 102 (2002) 2693–2724.

[10] A. Ohashi, H. Watarai, Azo-imine resonance in palladium(II)-pyridylazo complex adsorbed at liquid-liquid interfaces studied by centrifugal liquid membrane-resonance raman microprobe spectroscopy, Langmuir. 18 (2002) 10292–10297.

[11] S. Yamamoto, H. Watarai, Surface-Enhanced Raman Spectroscopy of Dodecanethiol-Bound Silver Nanoparticles at the Liquid/Liquid Interface, Langmuir. 22 (2006) 6562–6569.

[12] S.G. Booth, D.P. Cowcher, R. Goodacre, R.A.W. Dryfe, Electrochemical modulation of SERS at the liquid/liquid interface., Chem. Comm.. 50 (2014) 4482–4484.

[13] L. Poltorak, M. Dossot, G. Herzog, A. Walcarius, Interfacial processes studied by coupling electrochemistry at the polarised liquid-liquid interface with in situ confocal Raman spectroscopy, Phys. Chem. Chem. Phys. 16 (2014) 26955–26962.

[14] D.J. Fermin, H.D. Duong, Z. Ding, Ó. Brevet, H.H. Girault, Photoinduced electron transfer at liquid/liquid interfaces, Phys. Chem. Chem. Phys. 1 (1999) 1461–1467.

[15] R.M. Corn, H.H. Girault, H. Jin, D.J. Fermín, Marangoni flow in micro-channels, Electrochem. Commun. 1 (1999) 190–193.

[16] D. Ibañez, E.C. Romero, A. Heras, A. Colina, Dynamic Raman spectroelectrochemistry of single walled carbon nanotubes modified electrodes using a Langmuir-Schaefer method, Electrochim. Acta. 129 (2014) 171–176.

[17] D. Ibañez, C. Fernandez-Blanco, A. Heras, A. Colina, Time-Resolved Study of the Surface-Enhanced Raman Scattering Effect of Silver Nanoparticles Generated in Voltammetry Experiments., J. Phys. Chem. C. 118 (2014) 23426–23433.

[18] M. Muniz-Miranda, Surface enhanced Raman scattering and normal coordinate analysis of 1,10-phenanthroline adsorbed on silver sols, J. Phys. Chem. A. 104 (2000) 7803–7810.

[19] R. Mažeikiene, G. Niaura, A. Malinauskas, Electrochemical redox processes at cobalt hexacyanoferrate modified electrodes: An in situ Raman spectroelectrochemical study, J. Electroanal. Chem. 719 (2014) 60–71.

[20] D.T. Schwartz, S.M. Haight, Transport and chemistry at electroactive interfaces studied using line-imaging Raman spectroscopy, Colloids Surfaces A Physicochem. Eng. Asp. 174 (2000) 209–219.